LETTER

https://doi.org/10.1038/s41586-018-0238-4

A naturally occurring antiviral ribonucleotide encoded by the human genome

Anthony S. Gizzi[1,5], Tyler L. Grove[1,5]*, Jamie J. Arnold[2], Joyce Jose[2], Rohit K. Jangra[3], Scott J. Garforth[1], Quan Du[1], Sean M. Cahill[1], Natalya G. Dulyaninova[1], James D. Love[4], Kartik Chandran[3], Anne R. Bresnick[1], Craig E. Cameron[2] & Steven C. Almo[1,4]*

Viral infections continue to represent major challenges to public health, and an enhanced mechanistic understanding of the processes that contribute to viral life cycles is necessary for the development of new therapeutic strategies[1]. Viperin, a member of the radical *S*-adenosyl-L-methionine (SAM) superfamily of enzymes, is an interferon-inducible protein implicated in the inhibition of replication of a broad range of RNA and DNA viruses, including dengue virus, West Nile virus, hepatitis C virus, influenza A virus, rabies virus[2] and HIV[3,4]. Viperin has been suggested to elicit these broad antiviral activities through interactions with a large number of functionally unrelated host and viral proteins[3,4]. Here we demonstrate that viperin catalyses the conversion of cytidine triphosphate (CTP) to 3′-deoxy-3′,4′-didehydro-CTP (ddhCTP), a previously undescribed biologically relevant molecule, via a SAM-dependent radical mechanism. We show that mammalian cells expressing viperin and macrophages stimulated with IFNα produce substantial quantities of ddhCTP. We also establish that ddhCTP acts as a chain terminator for the RNA-dependent RNA polymerases from multiple members of the Flavivirus genus, and show that ddhCTP directly inhibits replication of Zika virus in vivo. These findings suggest a partially unifying mechanism for the broad antiviral effects of viperin that is based on the intrinsic enzymatic properties of the protein and involves the generation of a naturally occurring replication-chain terminator encoded by mammalian genomes.

Consideration of genome context shows that in vertebrates viperin is always immediately adjacent to a gene annotated as cytidylate monophosphate kinase 2 (*CMPK2*) and in some organisms, such as *Lacinutrix mariniflava*, these two genes are fused (Extended Data Fig. 1a). These observations suggested that viperin might modify a nucleotide. Evaluation of approximately 200 constructs derived from 8 mammalian species identified a *Rattus norvegicus* viperin (rVIP), including residues 51–361, which exhibited excellent properties in solution (Extended Data Fig. 1b, c). We screened rVIP against a diverse set of nucleotides and deoxynucleotides, looking for enhanced 5′-deoxyadenosine (5′-dA) formation as an indicator of substrate activation (See Supplementary Information for details). As with most other radical-SAM proteins, when provided with dithionite as an artificial electron donor rVIP performs reductive cleavage of SAM in the absence of substrates. As shown in Fig. 1a, CTP selectively activates 5′-dA production by approximately 130-fold relative to protein alone. Liquid chromatography shows that, in addition to 5′-dA (9.1 min), another product is present (5.2 min) (Fig. 1b), which exhibits a UV-visible spectrum similar to CTP ($\lambda_{max} = 271$ nm), indicating that the pyrimidine ring is not notably modified by the viperin-mediated reaction (Fig. 1c). Liquid chromatography coupled with mass spectrometry (LC–MS) showed the new compound exhibited a negative-ion mass to charge ratio ($-m/z$) of 464.1, which is 18 Da less than the $-m/z$ of 482.1 of CTP (Fig. 1d, e).

^{13}C–^{13}C correlation spectroscopy (COSY) NMR on uniformly labelled $^{13}C_9{}^{15}N_3$-viperin product, and ^{1}H–^{13}C 2D heteronuclear single quantum coherence (2D HSQC) chemical-shift analysis and ^{31}P NMR analysis on natural abundance viperin product were performed (see Supplementary Information for details, Extended Data Figs. 1d, 2; see Supplementary Table 1 for chemical-shift data). Taken together, all available NMR and mass spectrometry data are consistent with the rVIP-catalysed conversion of CTP to ddhCTP, in which dehydration—involving the loss of both the 4′ hydrogen and the 3′ hydroxyl group—occurs without rearrangement of the carbon skeleton. It is notable that MoaA, which catalyses the conversion of GTP to (8S)-3′,8-cyclo-7,8-dihydroguanosine 5′-triphosphate[5], is the enzyme with the highest sequence similarity to viperin for which an unambiguous functional annotation exists. Additionally, the recent report of the structure of viperin from *Mus musculus* proposed that the presumptive catalytic site shares high amino acid conservation with MoaA and may operate on a nucleotide-like substrate[6]. These observations are consistent with the above data.

rVIP has a K_m of 183 ± 28 μM for CTP and produces ddhCTP with a maximum velocity of 0.185 ± 0.007 min^{-1} (Fig. 1f). The intracellular concentration of CTP typically falls in the 1 mM range, which agrees well with the K_m obtained for rVIP for CTP[7], and the rate of ddhCTP formation is consistent with that of other radical-SAM enzymes with their native substrates[8]. 5′-dA and ddhCTP production is tightly coupled, with one molecule of 5′-dA generated for every ddhCTP (Extended Data Fig. 3a). rVIP also produces ddhCTP when the reaction is initiated by an enzymatic reducing system, indicating that dithionite does not direct an unanticipated side reaction between rVIP and CTP (Extended Data Fig. 3b).

A recent report described a radical-SAM enzyme from the thermophilic fungus *Thielavia terrestris* (58% sequence identity to human viperin) that was capable of catalysing the coupling of UDP–glucose and 5′-dA to generate an uncharacterized product with a *m/z of* 818.1[9]. In addition, a preliminary report suggested that viperin homologues from *Methanofollis liminatans* (archaea, 35% sequence identity to human viperin) and *Trichoderma virens* (fungi, 55% identity) catalyse the radical-based condensation of 5′-dA and isopentenyl pyrophosphate to yield adenylated isopentyl pyrophosphate[10]. Substrate activation and competition assays demonstrate that mammalian viperin does not catalyse these transformations (Fig. 1a, Extended Data Fig. 3c–f). We therefore conclude that UDP–glucose and isopentenyl pyrophosphate are not likely to be physiological substrates for mammalian viperins; although it remains a possibility that other eukaryotes use viperin homologues to perform distinct functions. Analogous competition experiments demonstrated that deoxyCTP is also not a substrate of rVIP (Extended Data Fig. 3g).

Incubation of rVIP with SAM and CTP deuterated at the 2′, 3′, 4′, 5′ and 5 positions (deuCTP), increased the $-m/z$ of 5′-dA from 250.1 to 251.1, consistent with the transfer of one deuterium from deuCTP to 5′-dA. Additionally, ddhCTP from this reaction exhibited a $-m/z$ of 468.1, indicating that the deuterium abstracted by 5′-dA did not return to the product (Extended Data Fig. 3h, i). Derivatives

[1]Department of Biochemistry, Albert Einstein College of Medicine, Bronx, NY, USA. [2]Department of Biochemistry and Molecular Biology, The Pennsylvania State University, University Park, PA, USA. [3]Department of Microbiology and Immunology, Albert Einstein College of Medicine, Bronx, NY, USA. [4]Institute for Protein Innovation, Boston, MA, USA. [5]These authors contributed equally: Anthony S. Gizzi, Tyler L. Grove. *e-mail: tyler.grove@einstein.yu.edu; steve.almo@einstein.yu.edu

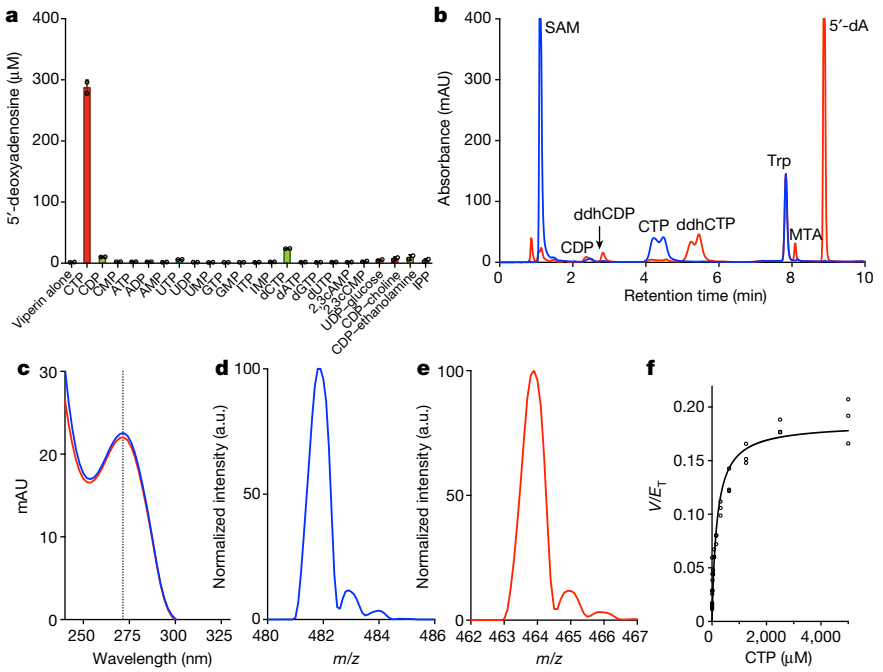

Fig. 1 | Substrate specificity of viperin. a, A panel of nucleotides was mixed with rVIP and SAM, and the resulting 5′-dA measured. Data are from two independent experiments. **b**, High-performance liquid chromatography analysis showing viperin-mediated conversion of CTP to a new product (time = 0, blue; time = 45 min, red). **c**, UV-visible spectrum of CTP (blue) and the new product (ddhCTP, red). Absorbance maximum at 271 nm (dotted line). **d**, **e**, Mass spectrometry for CTP (**d**, $-m/z = 482.1$) and ddhCTP (**e**, $-m/z = 464.1$). All results have been repeated at least three times. **f**, Kinetic analysis of rVIP with CTP: K_m for CTP = 182.8 ± 27.6 μM and V_{max} = 0.185 ± 0.007 min^{-1} (V/E_T, initial velocity of the reaction divided by the total enzyme concentration). Data are mean ± s.d. from three independent experiments.

of site-specifically deuterated CTP demonstrated that 5′-dA• initiates the reaction by uniquely abstracting the hydrogen from the 4′ position of CTP (see Supplementary Information for details, Extended Data Figs. 2, 4). On the basis of this observation, a provisional mechanism is outlined in Fig. 2d, in which viperin uses the 5′-dA• to abstract the hydrogen atom at the 4′ position of the ribose of CTP, subsequently allowing for the loss of the 3′-hydroxyl group with general acid assistance. The resulting resonance-stabilized radical cation is then reduced by one electron to yield the designated product. This mechanism has precedent from model studies of the radiolytic cleavage of single-stranded DNA, wherein generation of a 4′-deoxyribosyl radical causes heterolytic dissociation of the 3′ phosphate group, resulting in a 3′-cation-4′-yl radical[11]. The source of the additional electron needed to reduce intermediate three (or four) in the viperin-catalysed reaction is currently unclear. However, we propose that—similar to other radical-SAM enzyme reactions[12]—the electron probably derives from a reduced 4Fe–4S cluster, which suggests that viperin requires two electrons to complete each turnover: one to generate the 5′-dA• and another to reduce intermediate three (or four).

CMPK2 is always immediately adjacent to viperin in vertebrate genomes and is co-transcribed with viperin during IFN stimulation[13], suggesting a functional linkage. Human CMPK2 (hCMPK2) was previously reported to catalyse the ATP-dependent phosphorylation of the monophosphates CMP, UMP and dCMP to the corresponding diphosphates[14]. By contrast, we find that hCMPK2 exhibits strong preference for CDP and UDP as substrates, yielding CTP and UTP, respectively (Extended Data Fig. 5a). Notably, when provided with ddhCDP, hCMPK2 displayed a tenfold-lower activity for producing ddhCTP when compared to the rate of CTP and UTP formation (Extended Data Fig. 5a, Supplementary Table 2). Therefore, on the basis of the synteny and coordinated expression of viperin and CMPK2, and the available biochemical data, we propose that CMPK2 primarily functions to ensure sufficient substrate (that is, CTP produced from CDP, or by

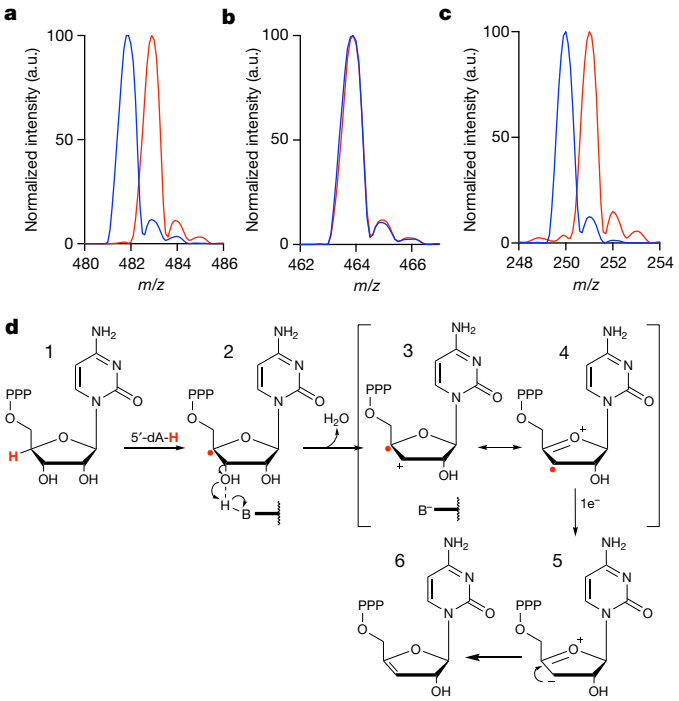

Fig. 2 | Proposed mechanism for formation of ddhCTP. a, m/z of CTP (blue) or 4′-^{2}H -CTP (red). **b**, Mass spectrometry of ddhCTP from reactions with either CTP (blue), or 4′-^{2}H -CTP (red) and rVIP. Deuterium from 4′-^{2}H -CTP is not retained in ddhCTP as products have the same $-m/z$ 464.1. **c**, 5′-dA derived from 4′-^{2}H -CTP (red trace) increases by one mass unit owing to the incorporation of deuterium. These experiments have been repeated at least three times with similar results. **d**, After hydrogen atom abstraction at the 4′ position of CTP, general base-assisted loss of the 3′ hydroxyl group leads to a carbocation/radical intermediate that is reduced by one electron to yield the ddhCTP product.

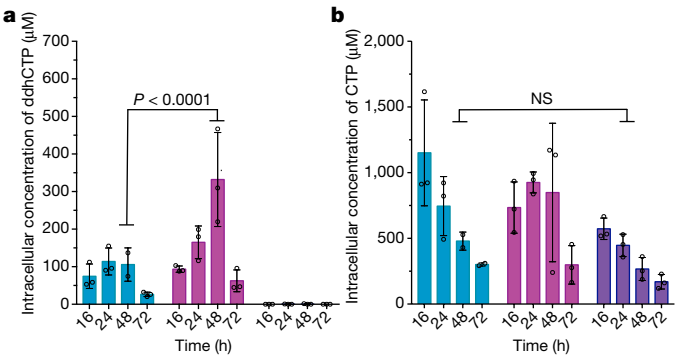

Fig. 3 | Expression of viperin in HEK293 cells produces ddhCTP. **a**, Cells expressing hVIP (aqua), hVIP and hCMPK2 (pink) or empty vector (purple). Analysis of ddhCTP formation indicates that the cells with hVIP and hCMPK2 cells show a statistically significant increase in ddhCTP formation over viperin alone 48 h after transfection. In cells with empty vector, ddhCTP levels were undetectable. **b**, Intracellular concentrations of CTP did not differ significantly over time. Data are mean ± s.d. from three biologically independent samples; *P* value is from a two-way ANOVA with Tukey's post hoc test. NS, not significant.

CTP synthetase acting on UTP) for viperin-mediated production of ddhCTP during viral infection.

To demonstrate that ddhCTP can be produced in mammalian cytosol, we generated a series of human viperin (hVIP) (83% identical to rVIP) and hCMPK2 expression constructs for transient transfection in HEK293T cells (Supplemenary Table 3, Extended Data Fig. 5b). As HEK293T cells do not express viperin in the presence or absence of IFN[15], ddhCTP production would not be expected in the absence of exogenous viperin expression. HEK293T cells were transfected with a control plasmid, hVIP alone, hCMPK2 alone or both hVIP and hCMPK2, and collected at defined times for LC–MS analysis (see Supplementary Information for details). In all cases, over a 72-h time course, the overall nucleotide pool consistently decreases, probably owing to limiting nutrient levels, though the overall growth and cell viability are not affected (Supplementary Table 4). In addition, at each time point there are no statistically significant differences in total nucleotide concentrations between the control, hVIP, and hVIP and hCMPK2 treated cells (Extended Data Fig. 6a–d). Notably, HEK293T cells transfected with control plasmid exhibited ddhCTP levels below our limit of detection of approximately 400 fmol (Fig. 3a, right), whereas HEK293T cells transfected with the hVIP plasmid exhibited high intracellular ddhCTP levels (approximately 75 μM at 16 h post-transfection) (Fig. 3a, left), which decreases to approximately 35 μM after 72 h. Cotransfection with hVIP and hCMPK2 plasmids resulted in an approximately fourfold increase in the amount of ddhCTP to approximately 330 μM at 48 h (Fig. 3a, middle, purple, $P < 0.0001$). Moreover, coexpression of hVIP and hCMPK2 causes the ratio of ddhCTP to CTP concentrations to increase over time, whereas overexpression of hVIP alone results in a constant ratio of ddhCTP to CTP (Extended Data Fig. 6e). This behaviour may enable viperin to continue generating ddhCTP even though roughly 30% of the total cellular pool of cytidine triphosphates is present as ddhCTP at 48 h. These observations demonstrate that in vivo viperin is essential for production of ddhCTP, and suggest that CMPK2 may function to ensure that CTP is not limiting in the presence of viperin.

It is well documented that viperin expression can be robustly induced in immune cells by interferon, lipopolysaccharide and double-stranded RNA analogues[16]. Therefore, we cultured immortalized murine macrophages (RAW264.7) in the presence or absence of IFNα in serum-free medium, as it has previously been shown that RAW264.7 cells express viperin in an IFNα-sensitive fashion[2]. When collected after 19 h, the concentration of ddhCTP was shown to be highly dependent on the concentration of IFNα (Extended Data Fig. 7a). RAW264.7 cells cultured in the presence of 250 ng ml^{-1} IFNα generated intracellular concentrations of ddhCTP reaching nearly 350 μM, whereas the intracellular concentrations of ATP, UTP and CTP were unaltered (Extended Data Fig. 7b). Analogous to the behaviour observed in HEK293T cells cotransfected with hVIP and hCMPK2, treatment of RAW264.7 cells with 250 ng ml^{-1} IFNα resulted in ddhCTP representing a sizable proportion (that is, 30%) of the total cytidine triphosphate pool (ddhCTP (approximately 350 μM) to CTP (approximately 800 μM)), whereas the level of CTP remained unchanged. This behaviour suggests that the viperin-mediated inhibition of viral replication is not a consequence of the limitation of the available pool of intracellular CTP, or other nucleotides, but rather is dependent on the generation of relevant concentrations of ddhCTP.

Because members of the flavivirus family are known to be sensitive to the catalytic activity of viperin[17], and because of the resemblance of ddhCTP to known polymerase chain terminators, we examined the effect of ddhCTP on dengue virus RNA-dependent RNA polymerase (RdRp) activity. First, we demonstrated that ddhCTP is a substrate for dengue virus RdRp using a primed-template assay[18] (Extended Data Fig. 8a, b). Addition of CTP, 3′-dCTP or ddhCTP led to incorporation of all of these nucleotides (Extended Data Fig. 8b). As expected, addition of UTP to the CMP-incorporated RNA led to further extension to the end of template (Extended Data Fig. 8b, c). However, addition of UTP to the 3′-dCMP- or ddhCMP-incorporated RNA did not support robust extension (Extended Data Fig. 8b, c), as expected for the action of chain terminators. A more stringent test of the effectiveness of a chain terminator is direct competition with natural ribonucleotides. Therefore, we evaluated RNA synthesis in the presence of increasing concentrations of ddhCTP or 3′-dCTP (Fig. 4a). Both ddhCTP and 3′-dCTP were incorporated and inhibited production of full-length RNA (Fig. 4a). Additionally, by titrating ddhCTP at different concentrations of CTP we determined the relative efficiency of the use of ddhCTP compared to CTP for dengue virus RdRp, as well as the RdRp from West Nile Virus (WNV), another pathogenic flavivirus (Fig. 4b, Extended Data Fig. 8e–j). This analysis yielded a 135- and 59-fold difference in the use of ddhCTP relative to CTP for dengue virus and WNV RdRps, respectively. We also evaluated two additional members of the flavivirus family, Zika virus (ZIKV) and hepatitis C virus RdRps. Both of these RdRps were susceptible to inhibition by ddhCTP utilization and chain termination (Fig. 4c, d), consistent with studies demonstrating the antiviral activity of viperin against these viruses[19–21]. These data suggest that the flavivirus RdRps would be susceptible to inhibition by ddhCTP during replication (Extended Data Fig. 9g). Given the efficiency of use and genome size, it is calculated that even a probability of incorporating the ddhCTP chain terminator during replication of approximately 1% would result in considerable reduction of full-length genomes (Extended Data Fig. 9g). To determine whether our observations with the flavivirus RdRps extend to RdRps from other supergroups, we evaluated members of supergroup I. Specifically, we used the RdRps from human rhinovirus type C (HRV-C) and poliovirus, which are both members of the picornavirus family (Extended Data Fig. 9). Direct-incorporation experiments revealed the use of both ddhCTP and 3′-dCTP by HRV-C RdRp (Extended Data Fig. 9b). However, in the presence of other rNTPs, both HRV-C and poliovirus RdRp were poorly inhibited by ddhCTP (Extended Data Fig. 9c–f), even though both are inhibited by 3′-dCTP. On the basis of this data, we conclude that not all RdRps are sensitive to ddhCTP, suggesting that different viruses will exhibit a range of susceptibilities to viperin expression in vivo.

The in vitro enzymatic characterizations suggest that ddhCTP would be sufficient for the in vivo inhibition of viral replication. First, we demonstrated that synthetic ddhC nucleoside was capable of traversing the plasma membrane of Vero and HEK293T cells and being metabolized to ddhCTP (1 mM synthetic ddhC resulted in the intracellular accumulation of 129 μM and 78 μM ddh-CTP after 24 h, respectively) (Extended Data Fig. 5c, d). Next, we used the historical African strain MR766 (Uganda 1947)[22] and two contemporary strains, PRVABC59 (Puerto Rico; 2015)[23] and R103451 (Honduras; 2016, GenBank:

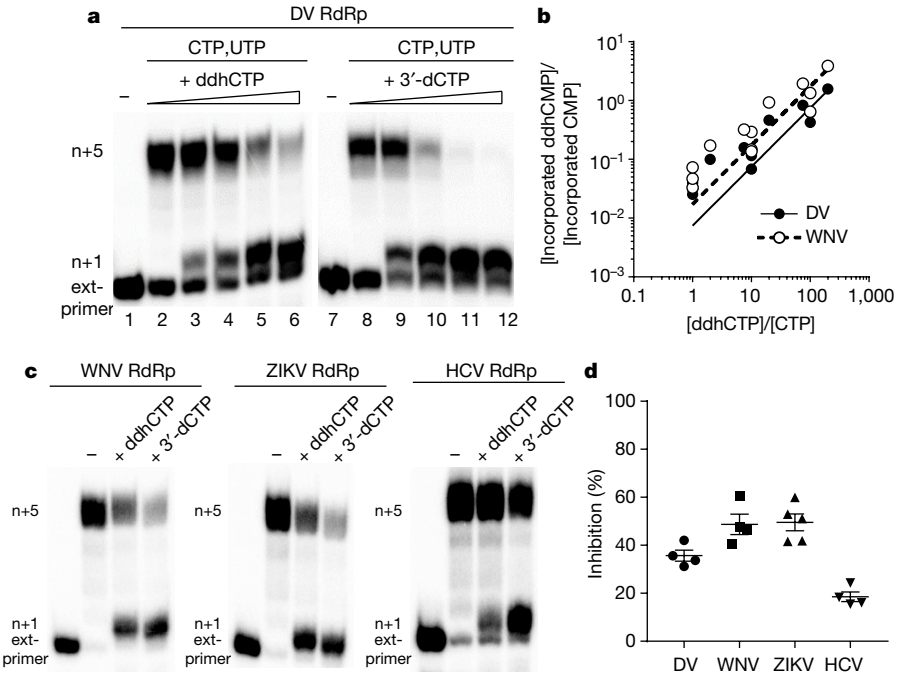

Fig. 4 | ddhCTP inhibits flavivirus RdRps by a chain termination mechanism. a, Primer extension assays show that ddhCTP (0, 1, 10, 100 and 300 μM) inhibits dengue virus (DV) RdRp. A trinucleotide is used to prime RNA synthesis in the presence of nucleotides (α^{32}P-NTPs) producing a 15-nt product that we refer to as extended primer (ext-primer). Additional incorporation of nucleotides leads to production of n + 1 and/or n + 5 product. Experiments repeated independently four times with similar results. **b**, Plot of [incorporated ddhCMP]/[incorporated CMP] versus [ddhCTP]/[CTP]. Data are fit to lines with slopes of 0.0074 ± 0.0006 (DV) and 0.017 ± 0.002 (WNV). At each ratio of [ddhCTP]/[CTP] a total of at least three independent experiments were preformed, with a total sample size of 24. **c**, Inhibition of the RdRp from WNV, ZIKV and hepatitis C virus (HCV) by either ddhCTP or 3′-dCTP (100 μM). Experiments repeated independently four to five times with similar results. **d**, Percentage of inhibition shown. Data are mean ± s.e.m. from four independent experiments. Gel shown in panel **c** was quantified by using ImageQuant TL software (GE).

KX262887), to evaluate the antiviral activity of ddhC towards ZIKV replication and release from Vero cells. Treatment with ddhC resulted in a reduction in ZIKV titres of one to two orders of magnitude, which was dependent on dose, multiplicity of infection (MOI), duration of infection and strain (Supplementary Table 5). For example, at a MOI of 0.1, we observed 50–200-fold reduction in viral titre for ZIKV MR766 at all time points (Fig. 5a), with reductions of 5–50-fold also observed at a MOI of 1.0 (Extended Data Fig. 10a). ZIKV R103451 (Honduras) and ZIKV PRVABC59 (Puerto Rico) exhibited analogous sensitivities to ddhC treatment (Supplementary Table 5, Extended Data Fig. 10a–c). The reduction in viral release was not a result of ddhC cytotoxicity, as incubation with 1 mM ddhC did not alter Vero cell viability (Fig. 5b, see Supplementary Information for details). These results, taken together with the in vitro enzymatic analyses, are consistent with a model in which ddhC-derived ddhCTP inhibits viral replication through premature chain termination of RdRp products.

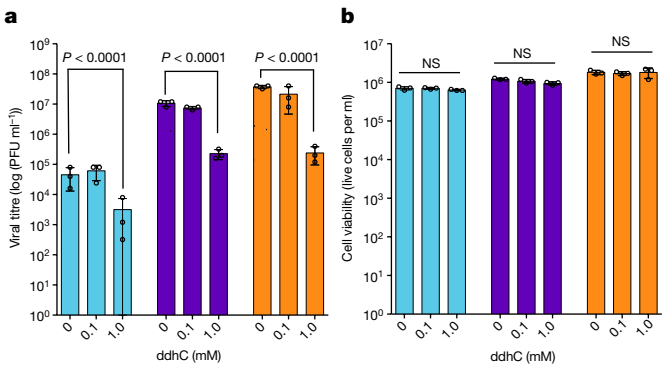

Fig. 5 | ddhC reduces ZIKV release in Vero cells. a, Vero cells were treated with increasing concentrations of ddhC for 24 h and infected with ZIKV MR766 (Uganda) at an MOI of 0.1. PFU, plaque-forming unit. **b**, For viability studies, Vero cells were treated with increasing concentrations of ddhC under the same culture conditions used for the antiviral experiment described in **a**. Data are mean ± s.d. from three biologically independent samples; *P* values are from a two-way ANOVA with Dunnett's post hoc analysis.

Of the hundreds of genes stimulated by IFN, most appear to function as negative effectors of viral activity, though their mechanisms of action remain to be defined. Here we propose a new paradigm for the antiviral function of viperin, which relies on its intrinsic catalytic activity to generate ddhCTP, a previously undescribed replication-chain terminator. To our knowledge, viperin is the only human protein that produces a small molecule capable of directly inhibiting viral replication machinery. Importantly, overexpression of viperin and production of ddhCTP does not appear to adversely affect the growth rate or viability of HEK293T or Vero cells. This observation indicates that the host RNA and DNA polymerases are not negatively affected by ddhCTP and have developed protective mechanisms to exclude incorporation or excise this compound during nucleic-acid synthesis; mechanistic studies on the use of ddhCTP by host polymerases will be an important area for future investigation. In addition to its inhibitory effect on viral RdRp activity, it is possible that viperin possesses additional antiviral functions. For example, despite reports that HRV infection induces viperin expression, ddhCTP does not appear to act as an effective chain terminator for the HRV RdRp[24]. Furthermore, in the case of human cytomegalovirus, viperin expression results in enhanced infectivity, possibly through alterations in cellular metabolism and disruption of the actin cytoskeleton[25]. It is probable that different pathogens are responsive to distinct subsets of the IFN-inducible genes and—given the range of modulatory effects it has on viruses—that viperin synergizes with other host- and pathogen-encoded genes.

Data availability

All data supporting the conclusions of the paper are available on reasonable request from the authors.

Online content

Any Methods, including any statements of data availability and Nature Research reporting summaries, along with any additional references and Source Data files, are available in the online version of the paper at https://doi.org/10.1038/s41586-018-0238-4.

Received: 17 July 2017; Accepted: 27 April 2018;
Published online 20 June 2018.

1. Molinari, N. A. M. et al. The annual impact of seasonal influenza in the US: measuring disease burden and costs. *Vaccine* **25**, 5086–5096 (2007).
2. Tang, H. B. et al. Viperin inhibits rabies virus replication via reduced cholesterol and sphingomyelin and is regulated upstream by TLR4. *Sci. Rep.* **6**, 30529 (2016).
3. Helbig, K. J. & Beard, M. R. The role of viperin in the innate antiviral response. *J. Mol. Biol.* **426**, 1210–1219 (2014).
4. Seo, J. Y., Yaneva, R. & Cresswell, P. Viperin: a multifunctional, interferon-inducible protein that regulates virus replication. *Cell Host Microbe* **10**, 534–539 (2011).
5. Hover, B. M., Loksztejn, A., Ribeiro, A. A. & Yokoyama, K. Identification of a cyclic nucleotide as a cryptic intermediate in molybdenum cofactor biosynthesis. *J. Am. Chem. Soc.* **135**, 7019–7032 (2013).
6. Fenwick, M. K., Li, Y., Cresswell, P., Modis, Y. & Ealick, S. E. Structural studies of viperin, an antiviral radical SAM enzyme. *Proc. Natl Acad. Sci. USA* **114**, 6806–6811 (2017).
7. Kennedy, A. D. et al. Complete nucleotide sequence analysis of plasmids in strains of *Staphylococcus aureus* clone USA300 reveals a high level of identity among isolates with closely related core genome sequences. *J. Clin. Microbiol.* **48**, 4504–4511 (2010).
8. Yokoyama, K., Numakura, M., Kudo, F., Ohmori, D. & Eguchi, T. Characterization and mechanistic study of a radical SAM dehydrogenase in the biosynthesis of butirosin. *J. Am. Chem. Soc.* **129**, 15147–15155 (2007).
9. Honarmand Ebrahimi, K. et al. The radical-SAM enzyme Viperin catalyzes reductive addition of a 5′-deoxyadenosyl radical to UDP-glucose *in vitro*. *FEBS Lett.* **591**, 2394–2405 (2017).
10. Lee, H. *A Proposed Mechanism for the Radical SAM Enzyme Viperin*. BSc thesis, Univ. of Illinois (2017).
11. Giese, B., Beyrich-Graf, X., Erdmann, P., Petretta, M. & Schwitter, U. The chemistry of single-stranded 4′-DNA radicals: influence of the radical precursor on anaerobic and aerobic strand cleavage. *Chem. Biol.* **2**, 367–375 (1995).
12. Grove, T. L. et al. A substrate radical intermediate in catalysis by the antibiotic resistance protein Cfr. *Nat. Chem. Biol.* **9**, 422–427 (2013).
13. Kambara, H. et al. Negative regulation of the interferon response by an interferon-induced long non-coding RNA. *Nucleic Acids Res.* **42**, 10668–10680 (2014).
14. Xu, Y., Johansson, M. & Karlsson, A. Human UMP-CMP kinase 2, a novel nucleoside monophosphate kinase localized in mitochondria. *J. Biol. Chem.* **283**, 1563–1571 (2008).
15. Teng, T. S. et al. Viperin restricts chikungunya virus replication and pathology. *J. Clin. Invest.* **122**, 4447–4460 (2012).
16. Wang, B. et al. Viperin is induced following toll-like receptor 3 (TLR3) ligation and has a virus-responsive function in human trophoblast cells. *Placenta* **36**, 667–673 (2015).
17. Jiang, D. et al. Identification of five interferon-induced cellular proteins that inhibit West Nile virus and dengue virus infections. *J. Virol.* **84**, 8332–8341 (2010).
18. Van Slyke, G. A. et al. Sequence-specific fidelity alterations associated with West Nile virus attenuation in mosquitoes. *PLoS Pathog.* **11**, e1005009 (2015).
19. Panayiotou, C. et al. Viperin restricts Zika virus and tick-borne encephalitis virus replication by targeting NS3 for proteasomal degradation. *J. Virol.* **92**, e02054-17 (2018).
20. Szretter, K. J. et al. The interferon-inducible gene viperin restricts West Nile virus pathogenesis. *J. Virol.* **85**, 11557–11566 (2011).
21. Wang, S. et al. Viperin inhibits hepatitis C virus replication by interfering with binding of NS5A to host protein hVAP-33. *J. Gen. Virol.* **93**, 83–92 (2012).
22. Dick, G. W., Kitchen, S. F. & Haddow, A. J. Zika virus. I. Isolations and serological specificity. *Trans. R. Soc. Trop. Med. Hyg.* **46**, 509–520 (1952).
23. Lanciotti, R. S., Lambert, A. J., Holodniy, M., Saavedra, S. & Signor, L. d. C C. Phylogeny of Zika Virus in Western hemisphere, 2015. *Emerg. Infect. Dis.* **22**, 933–935 (2016).
24. Proud, D. et al. Gene expression profiles during *in vivo* human rhinovirus infection: insights into the host response. *Am. J. Respir. Crit. Care Med.* **178**, 962–968 (2008).
25. Seo, J. Y. & Cresswell, P. Viperin regulates cellular lipid metabolism during human cytomegalovirus infection. *PLoS Pathog.* **9**, e1003497 (2013).

Acknowledgements We thank S. J. Booker for helpful discussions, L. Nordstroem (Chemical Synthesis & Biology Core Facility) for synthesis of ddhC and R. Sharma and J. Perryman for assistance with construction of RdRp expression plasmids and purification of RdRp enzymes. This work was supported by National Institutes of Health (NIH) Grants R21-AI133329 (T.L.G. and S.C.A.), P01-GM118303-01 (J. A. Gerlt and S.C.A.), U54-GM093342 (J. A. Gerlt and S.C.A.), U54-GM094662 (S.C.A.), R01-AI045818 (C.E.C.), Pennsylvania State University Start-Up Funds (J.J.), and the Price Family Foundation (S.C.A.). We acknowledge the Albert Einstein Anaerobic Structural and Functional Genomics Resource (http://www.nysgxrc.org/psi3/anaerobic.html).

Author contributions A.S.G., T.L.G., J.J.A., C.E.C. and S.C.A. designed the research; A.S.G. and T.L.G. contributed equally; A.S.G. and T.L.G. prepared protein and performed experiments; J.J.A. performed polymerase biochemistry; J.J. performed ZIKV release assays; Q.D. prepared isotopologues; R.K.J. and K.C. provided advice on virologic experiments and performed statistical analysis; S.M.C. performed NMR measurements; S.J.G. prepared HEK293T cells; N.G.D. prepared RAW264.7 cells; all authors analysed data. T.L.G., J.D.L., A.R.B., C.E.C. and S.C.A. supervised research. A.S.G., T.L.G., J.J.A., C.E.C. and S.C.A. wrote the manuscript.

Competing interests A.S.G., T.L.G., J.J.A., C.E.C. and S.C.A. are co-inventors on a U.S. provisional patent application (No. 62/548,425; filed by S.C.A.) that incorporates discoveries described in this manuscript.

Additional information
Extended data is available for this paper at https://doi.org/10.1038/s41586-018-0238-4.
Supplementary information is available for this paper at https://doi.org/10.1038/s41586-018-0238-4.
Reprints and permissions information is available at http://www.nature.com/reprints.
Correspondence and requests for materials should be addressed to T.L.G. or S.C.A.
Publisher's note: Springer Nature remains neutral with regard to jurisdictional claims in published maps and institutional affiliations.

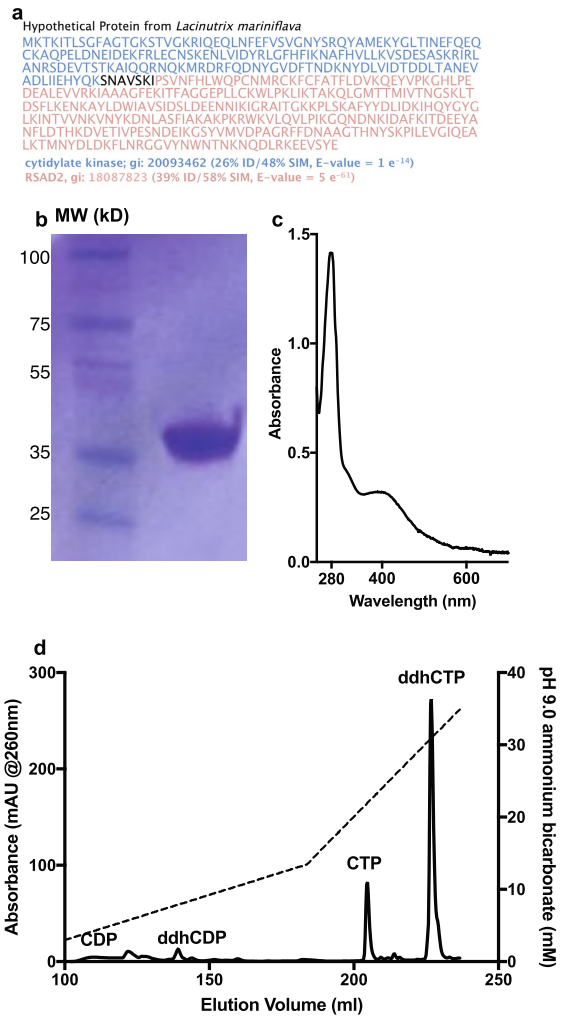

Extended Data Fig. 1 | Purification of rVIP and ddhCTP. a, Amino acid sequence from a *Lacinutrix mariniflava* fusion gene product of CMPK2- and a viperin-like protein. **b**, SDS–PAGE analysis after affinity and size-exclusion chromatography. The protein corresponding to amino acid residues 51–361 has a predicted molecular mass of 38.36 kDa. This construct was chosen because approximately 100 mg of protein could be purified from a 2-l fermentation. In addition, the protein is soluble at concentrations greater than 2 mM. **c**, UV-visible spectrum of purified rVIP (29.5 μM, UV 280/400 ratio of 4.2). **d**, Purification of ddhCTP using ammonium bicarbonate pH 9, with an elution gradient (dashed line) from 0.2 M to 0.8 M over 200 column volumes. All results have been repeated at least three times.

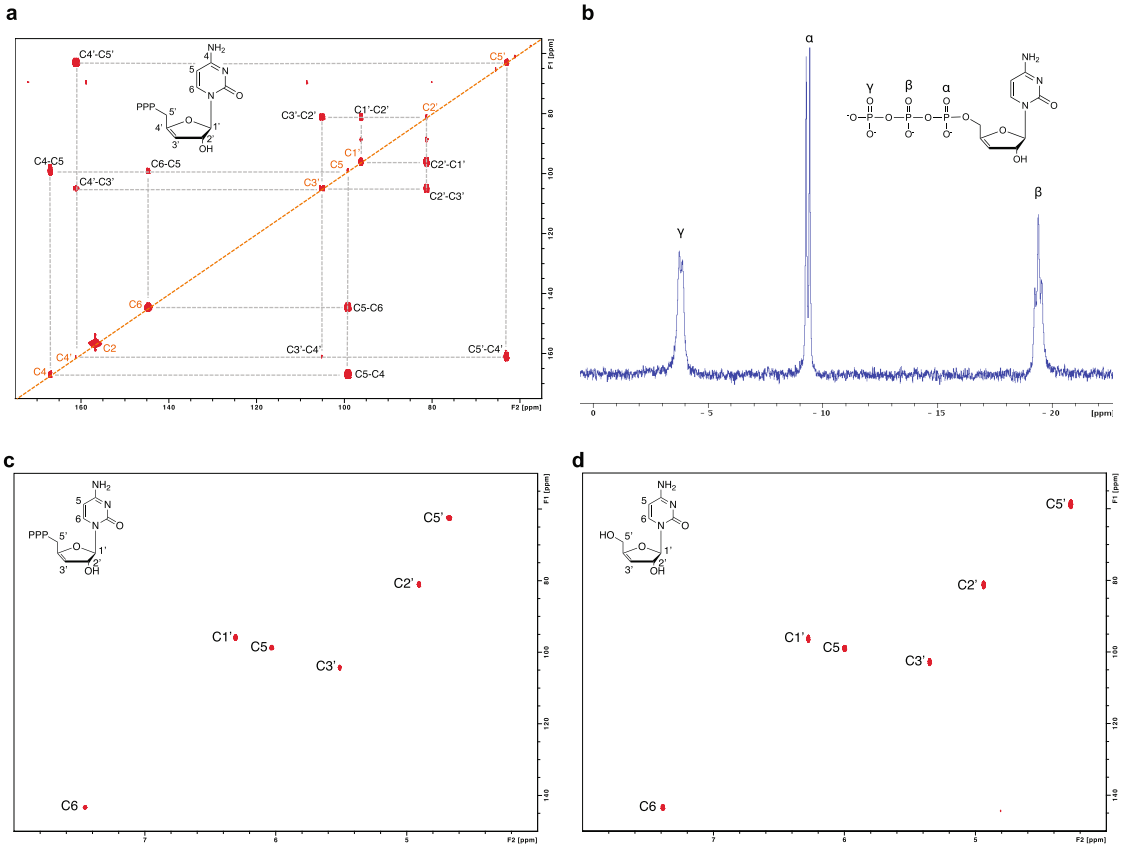

Extended Data Fig. 2 | NMR spectroscopy of ddhCTP. a, ^{13}C–^{13}C COSY spectrum of $^{13}C_9{}^{15}N_3$–ddhCTP. The assignments for the observed correlations of the ^{13}C-connectivities are indicated with the grey dotted lines. **b**, ^{31}P NMR spectra (300 MHz) of ddhCTP (1 mM) in D_2O at 300 K. Three resonance peaks at –19.5 (triplet), −9.5 (doublet) and –3.9 (doublet) p.p.m. correspond to the beta, alpha and gamma phosphates of ddhCTP, respectively. **c**, 2D-HSQC NMR spectra collected on purified 1 mM ddhCTP in D_2O. **d**, 2D-HSQC NMR spectra collected on 1 mM synthetic ddhC in D_2O. All experiments have been repeated twice.

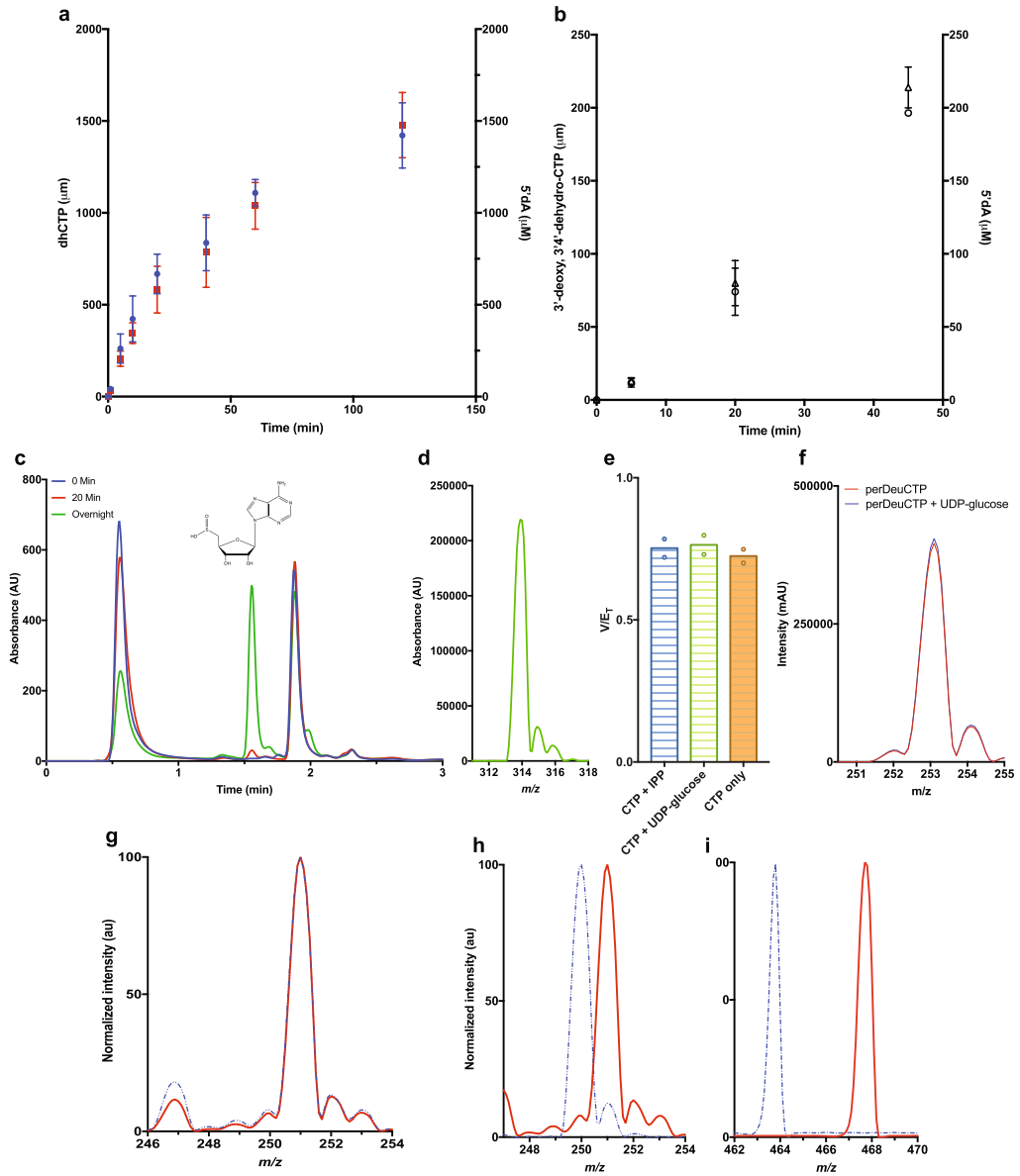

Extended Data Fig. 3 | rVIP produces a 1:1 stoichiometry of 5′-dA and ddhCTP and reacts specifically with CTP. a, Formation of ddhCTP (red squares) and 5′-dA (blue circles) from CTP and SAM in the presence of dithionite and 100 μM rVIP. ddhCTP is formed at roughly stoichiometric amounts with that of 5′-dA. Data are mean ± s.d. from three replicates. **b**, Formation of ddhCTP (open triangle,) and 5′-dA (open circle) from CTP and SAM in the presence of the flavodoxin, flavodoxin reductase and NADPH using 100 μM rVIP. Data are mean ± s.d. from three replicates. ddhCTP and 5′-dA are formed at roughly stoichiometric concentrations. The production of ddhCTP by this enzyme-driven reducing system indicates that ddhCTP formation is not the consequence of a side reaction with dithionite. **c**, High-performance liquid chromatography analysis (0 min, blue trace; 20 min, red trace; 12 h, green trace) showing the generation of a new peak at 1.55 min in the 12 h sample corresponding to a 5′-dA–dithionite adduct in the presence of 100 μM rVIP, 1 mM SAM and 10 mM IPP. **d**, Corresponding mass spectra in ESI negative mode of the peak occurring at 1.55 min in the 12 h sample. The 5′-dA–dithionite conjugate was calculated to have an exact mass of 315 Da and an *m*/*z* of 314.1. These results have been repeated twice. **e**, The rate of 5′-dA formed by 100 μM rVIP in the presence of 1 mM SAM and 1 mM CTP alone or 1 mM CTP with 10 mM IPP or UDP–glucose. Data are mean ± s.d. from three independent experiments. **f**, Mass spectrum traces of 5′-dA by ESI+. Reactions were conducted with 100 μM rVIP, 1 mM SAM and 1mM deuCTP with or without 10 mM UDP–glucose. The mass spectrum of 5′-dA produced during these reactions shows only the presence of deuterium, which derives from deuCTP, even when UDP–glucose is present at a tenfold higher concentration. An *m*/*z* of 252.1 represents the natural abundance peak of 5′-dA, an *m*/*z* of 253.1 indicating the addition of one deuterium. **g**, Mass spectrum trace showing –*m*/*z* of 5′-dA formed by combining 100 μM rVIP with 1 mM deuCTP (dotted blue trace) or 1 mM deuCTP with 1 mM deoxyCTP (red trace). The *y*-axis of each spectrum was normalized to 100% with arbitrary units (au) to enable direct comparison between each sample. The 5′-dA produced during this reaction has an *m*/*z* of 251.1, which is only consistent with rVIP abstracting a deuteron from deuCTP and not acting on the deoxyCTP (that is, lack of *m*/*z* 250.1). **h**, **i**, Mass spectrum trace showing –*m*/*z* of 5′-dA (**h**) or the new product (**i**), formed by combining 100 μM rVIP with either 1 mM CTP (dotted blue trace) or 1 mM deuCTP (red trace). When rVIP was incubated with SAM and CTP deuterated at the 2′, 3′, 4′, 5′ and 5 positions (deuCTP), the −*m*/*z* of 5′-dA increased from 250.1 to 251.1, consistent with the transfer of one deuterium from deuCTP to 5′-dA•. When ddhCTP from the reaction was analysed by mass spectormetry, the product exhibited a −*m*/*z* of 468.1, indicating that the deuterium abstracted by 5′-dA during catalysis did not return to the product. The *y*-axis of each spectrum was normalized to 100% with arbitrary units (au) to enable direct comparison between each sample. These results have been repeated at least twice.

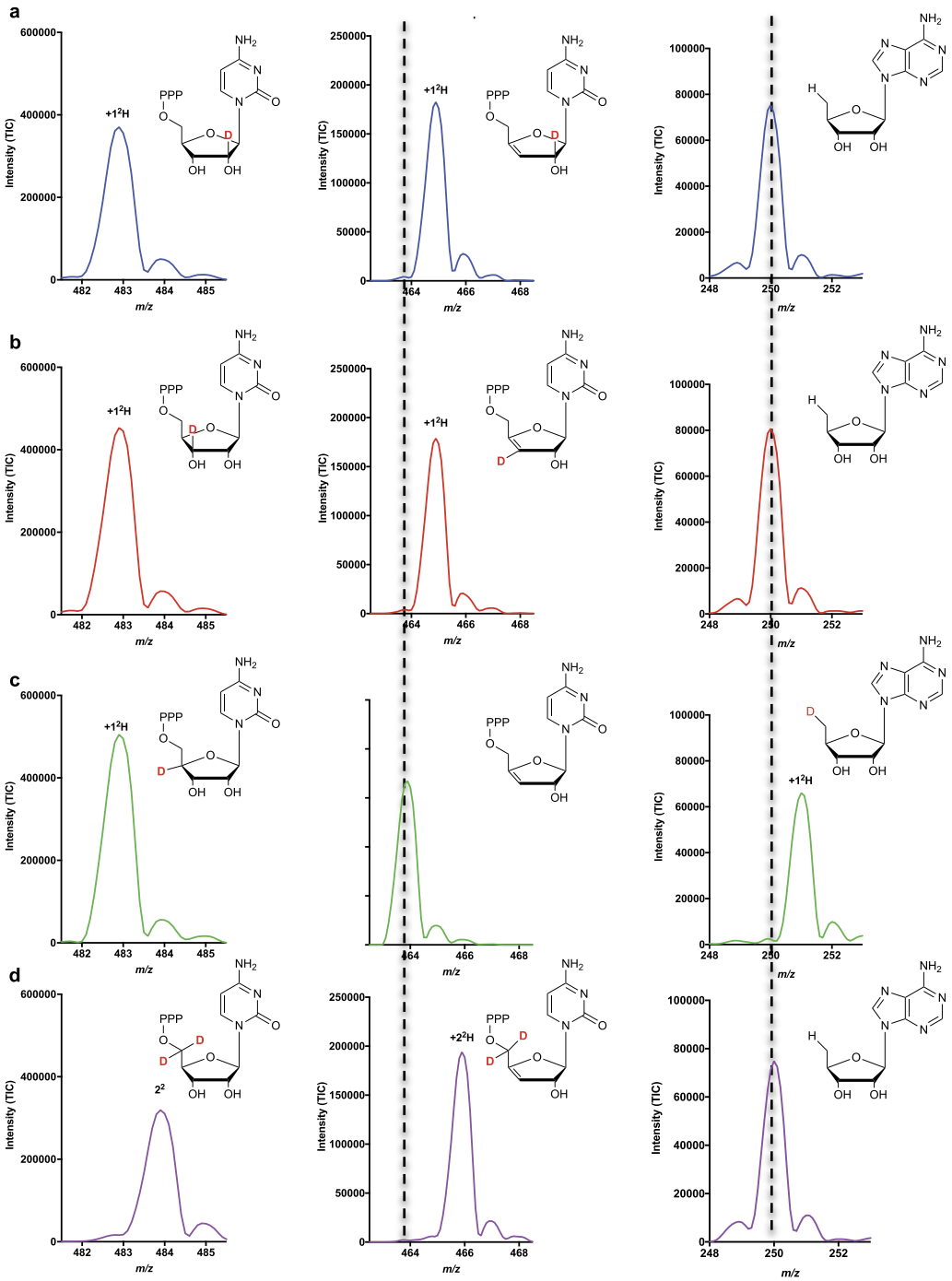

Extended Data Fig. 4 | Viperin abstracts the 4′-H from CTP. a–d, Using CTP with deuterium (^{2}H denoted with a red D) incorporated at either the 2′-^{2}H (**a**), 3′-^{2}H (**b**), 4′-^{2}H (**c**) or 5′-^{2}H$_2$ (**d**) (left column), we were able to monitor the loss of deuterium from the resulting product (middle column) and gain of a deuterium in the resulting 5′-dA (right column). The 5′-dA –*m*/*z* increases by one only in reactions containing CTP with a 4′-^{2}H (**c**, right column). Natural abundance peaks are denoted with dashed vertical lines. All experiments were repeated twice.

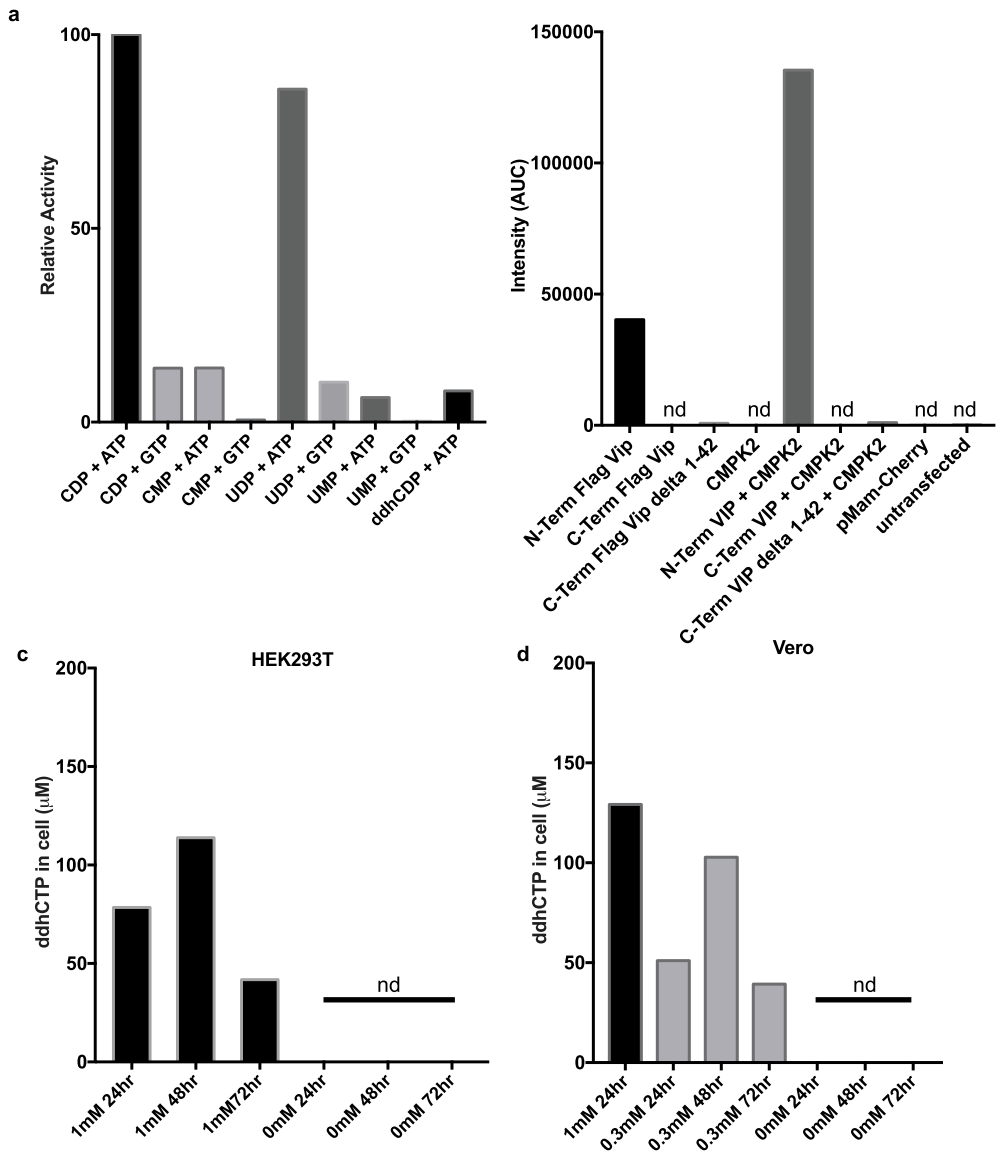

Extended Data Fig. 5 | CMPK2 phosphorylates UDP or CDP and synthetic ddhC can be converted to ddhCTP by cellular machinery. **a**, Formation of trinucleotide species (UTP, CTP or ddhCTP) from mono- and diphosphate species (1 mM UMP, UDP, CMP, CDP and ddhCDP) in the presence of either ATP or GTP as the phosphate donor by 5 μM hCMPK2. **b**, ddhCTP formation in HEK293T cells expressing either Flag–hVIP (N- or C-terminal tags), Flag–hVIP without the N-terminal amphipathic region (delta 1–42), hCMPK2 only, Flag–hVIP (N- or C-terminal tags) and hCMPK2, Flag–hVIP without the N-terminal amphipathic region (delta 1–42) and hCMPK2, a control plasmid or cells only. Only when the tag is on the N terminus of the full-length hVIP is ddhCTP produced at detectable levels. **c**, ddhCTP concentrations from HEK293T suspension cells that were incubated with synthetic ddhC (0 or 1 mM) for 24, 48 or 72 h (see Supplementary Information for details). **d**, ddhCTP concentrations from adherent Vero cells that were incubated with synthetic ddhC (0, 0.3 or 1 mM) for 24, 48 or 72 h (see Supplementary Information for details). All experiments were repeated once. nd, not detectable.

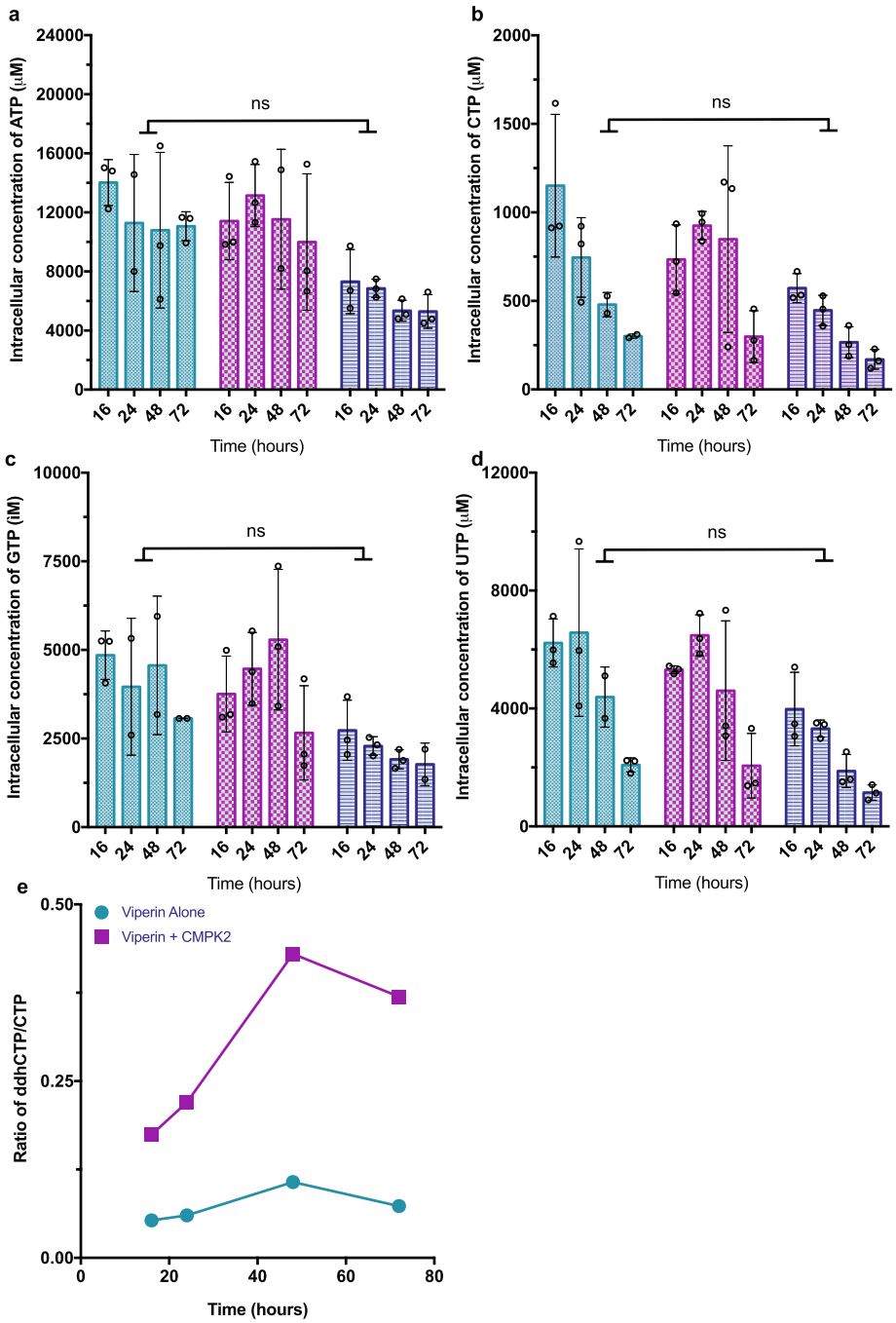

Extended Data Fig. 6 | Cellular concentrations of nucleotides are not affected by viperin expression. a–d, HEK293T cells expressing Flag–hVIP (aqua), Flag–hVIP and hCMPK2 (purple) or cells only (dark blue). Samples were taken at 16, 24, 48 and 72 hours post infection (h.p.i.). Extraction performed with a mixture of acetonitrile, methanol and water (40:40:20 and 0.1 M formic acid). Cellular concentrations were determined using $^{13}C_9{}^{15}N_{15}$–CTP, $^{13}C_{10}{}^{15}N_{10}$–ATP, $^{13}C_{10}N_5$–GTP and $^{13}C_9{}^{15}N_2$–UTP spiked into the extraction mixture at known concentrations and using equations (1) and (2) in Supplementary Information. Analysis of nucleotides ATP (**a**), CTP (**b**), GTP (**c**) and UTP (**d**) did not show statistically significant differences (ns) between Flag–hVIP, Flag–hVIP and hCMPK2 or cells only for any time point. Data are from three biologically independent samples. Statistical significance was determined using a two-way ANOVA (Supplementary Tables 12, 13, 14 and 15). **e**, Ratio of cellular concentrations of ddhCTP to CTP from HEK293T cells expressing Flag–hVIP (aqua) or Flag–hVIP and hCMPK2 (purple); samples were taken at 16, 24, 48 and 72 h post transfection. The overall ratio of ddhCTP to CTP remains constant when only Flag–hVIP is expressed, but the concentration of ddhCTP is boosted significantly relative to CTP when both Flag–hVIP and hCMPK2 are co-expressed (plots are derived from data shown in **c** and Fig. 3a).

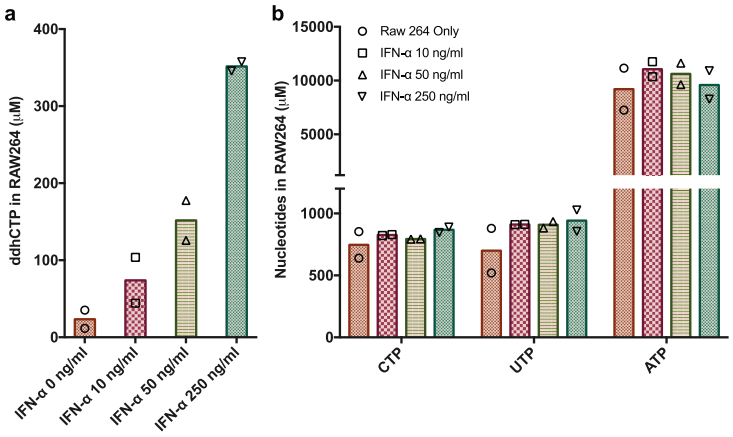

Extended Data Fig. 7 | Nucleotide concentrations are not affected during ddhCTP production. a, **b**, Concentrations of ddhCTP (**a**) and CTP, UTP and ATP (**b**) in immortalized macrophage cells (RAW 264.7) grown in serum-free medium in the presence of increasing concentrations of murine IFNα (10 ng ml^{-1}, 50 ng ml^{-1} and 250 ng ml^{-1}). Data are from two biologically independent samples.

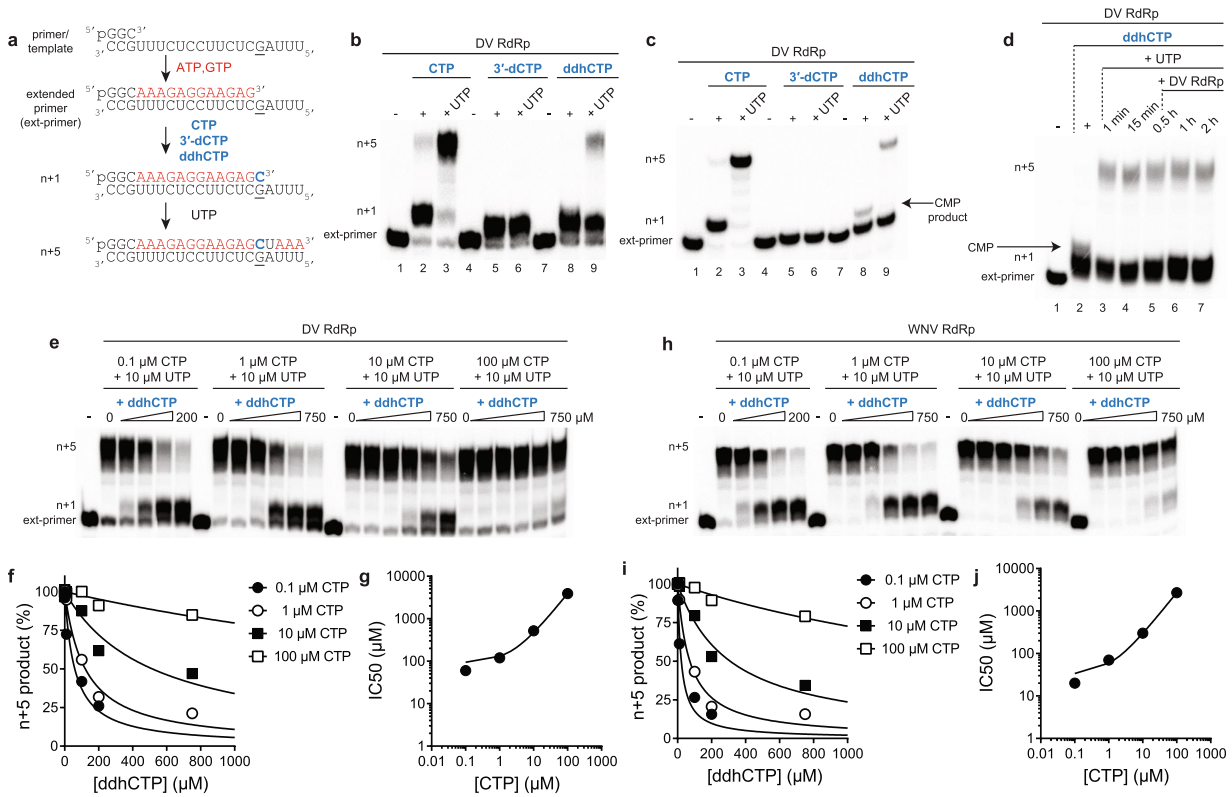

Extended Data Fig. 8 | ddhCTP is used as a substrate by dengue virus and WNV RdRp and chain terminates RNA synthesis. a, Schematic of primer-extension assay for evaluating dengue virus and WNV RdRp activity. **b**, Dengue virus RdRp-catalysed nucleoside incorporation using CTP, 3′-dCTP or ddhCTP as nucleoside triphosphate substrates. Some full-length product was observed in the presence of ddhCTP (more than 99% pure), which is due to residual contaminating CTP that could not be removed. **c**, Reaction products resolved by denaturing PAGE containing 40% formamide showing the trace amount of CTP contaminate in the ddhCTP preparation. These experiments were repeated independently at least four times with similar results. **d**, Longer incubation times and more dengue virus RdRp enzyme does not increase the yield of extended product. **e**, Dengue virus RdRp-catalysed nucleoside incorporation with increasing concentrations of ddhCTP (0, 1, 10, 100, 200 and 750 μM) at varying concentrations of CTP. This experiment was repeated independently three times with similar results. **f**, Plot of the percentage inhibition as a function of ddhCTP concentration at varying concentrations of CTP. Data were fit to a dose–response curve to obtain half-maximum inhibitory concentration (IC_{50}) values of ddhCTP of 60 ± 10, 120 ± 20, 520 ± 90 and 3,900 ± 700 μM at 0.1, 1, 10 and 100 μM CTP, respectively. This experiment was repeated at least three times with similar results. The total sample size is 24. The error reported is the standard error from the fit of the data to a dose–response curve. **g**, Plot of IC_{50} values as a function of CTP concentration. The data were fit to a line with a slope of 38 ± 1 and an intercept of 91 ± 25. The error reported is the standard error from the fit of the data to a line. **h**, WNV RdRp-catalysed nucleoside incorporation with increasing concentrations of ddhCTP (0, 1, 10, 100, 200 and 750 μM) at varying concentrations of CTP. This experiment was repeated at least three times with similar results. **i**, Plot of the percentage inhibition as a function of ddhCTP concentration at varying concentrations of CTP. Data were fit to a dose–response curve to obtain IC_{50} values of ddhCTP of 20 ± 10, 70 ± 10, 300 ± 40 and 2,700 ± 300 μM at 0.1, 1, 10 and 100 μM CTP, respectively. The total sample size is 24. The error reported is the standard error from the fit of the data to a dose–response curve. **j**, Plot of IC_{50} values as a function of CTP concentration. The data were fit to a line with a slope of 27 ± 1 and an intercept of 31 ± 8. Both of these results demonstrate that once ddhCMP is incorporated, it effectively terminates synthesis and that the small amount of extended product is from a trace amount of CTP contamination. The error reported is the standard error from the fit of the data to a line.

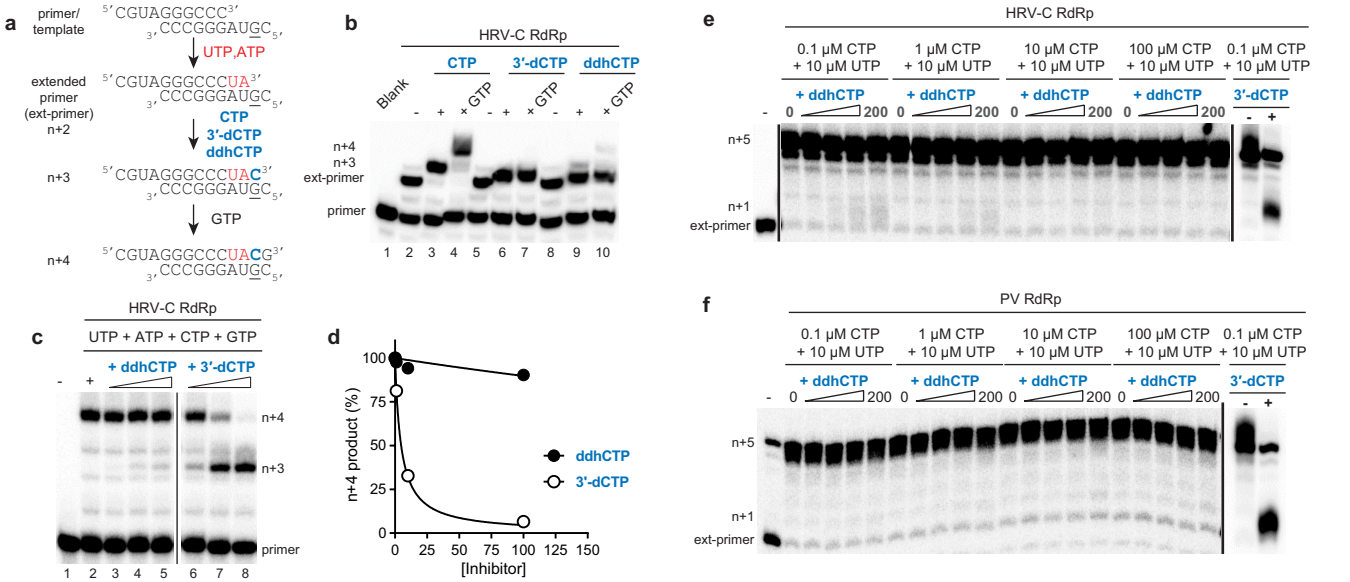

g

RdRp	IC50[a]	Probability[b]	% full-length genome[c]
DV RdRp	3×10^{4}	0.011	3×10^{-11}
WNV RdRp	2×10^{4}	0.015	4×10^{-17}
HRV-C RdRp	3×10^{6}	1×10^{-4}	86
PV RdRp	$\geq 3 \times 10^{7}$	$\geq 1 \times 10^{-5}$	99

Extended Data Fig. 9 | HRV-C and poliovirus RdRp are poorly inhibited by ddhCTP. a, Schematic of primer extension assay for evaluating HRV-C RdRp activity. **b**, HRV-C RdRp-catalysed nucleoside incorporation using CTP, 3′-dCTP or ddhCTP as nucleoside triphosphate substrates. These experiments were repeated independently at least four times with similar results. **c**, Increasing concentrations of ddhCTP does not efficiently inhibit HRV-C RdRp-catalysed RNA synthesis. HRV-C RdRp-catalysed nucleoside incorporation in the presence of increasing concentrations of either ddhCTP or 3′-dCTP. These experiments were repeated independently at least five times with similar results. **d**, Plot of the percentage inhibition as a function of either ddhCTP or 3′-dCTP concentration. Data were fit to a dose–response curve to obtain IC_{50} values of 900 ± 300 μM for ddhCTP and 5 ± 1 μM for 3′-dCTP. The total sample size is eight. The error reported is the standard error from the fit of the data to a dose–response curve. **e**, **f**, HRV-C (**e**) and poliovirus (**f**) RdRp-catalysed nucleoside incorporation with increasing concentrations of ddhCTP (0, 1, 10, 100 and 200 μM) at varying concentrations of CTP. Reactions were performed with the trinucleotide primer, 5′-pGGC, and 20-nt RNA template as described for dengue virus and WNV RdRp to directly compare results with HRV-C and poliovirus RdRp. At the highest concentration of ddhCTP, only approximately 2% inhibition was observed for HRV-C RdRp at 0.1 and 1 μM CTP. The IC_{50} values at 0.1 and 1 μM CTP are estimated to be approximately 10,000 and 20,000 μM ddhCTP, respectively. These values are three orders of magnitude higher than those obtained for dengue virus and WNV RdRp. Reactions in the presence of 3′-dCTP (200 μM) are shown as a control for inhibition. These experiments were repeated independently at least four times with similar results. **g**, Efficiency of incorporation and inhibition of viral RdRps. Footnotes: [a]Calculated for ddhCTP in direct competition with CTP (800 μM) using the linear equations obtained from the fit of the data shown in **g** and **j**. For HRV-C, the IC_{50} value was estimated to be two orders magnitude greater than that calculated for dengue virus and WNV RdRps as evidenced from the data shown in **d**. [b]Calculated for a ddhCTP concentration of 350 μM using the following equation: probability = [ddhCTP]/([ddhCTP] + IC_{50}). [c]Calculated using the following equation: $\text{full} - \text{length genome}(\%) = 100 \times (1 - \text{probability})^{C_n}$; in which C_n is the number of cytidine residues in the viral genome with values of 2,200, 2,497, 1,565 and 1,737 for dengue virus, WNV, HRV-C and poliovirus respectively.

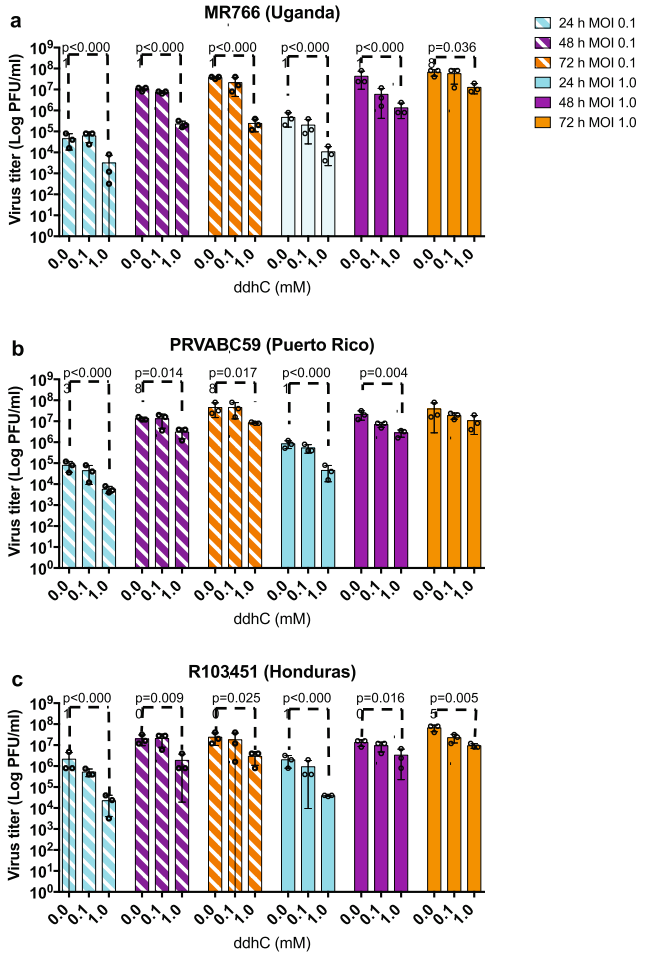

Extended Data Fig. 10 | ddhC reduces virus release of three different ZIKV isolates. Vero cells were treated with different concentrations of ddhC (0, 0.1 and 1 mM) for 24 h. After this 24-h period, the medium over cells was removed and cells were infected with fresh medium that contained the original concentrations of ddhC (0, 0.1 and 1 mM) and one of three strains of ZIKV; African strain MR766 (Uganda 1947), PRVABC59 (Puerto Rico; 2015) or R103451 (Honduras; 2016, GenBank: KX262887). After three hours of ZIKV infection, virus inoculum was removed and cells were treated with fresh medium that contained the original concentrations of ddhC (0, 0.1 and 1 mM). Virus samples were collected and the medium over cells was replaced with fresh medium that contained the original concentrations of ddhC at 24, 48 and 72 h.p.i. Viral titres at 24, 48 and 72 h.p.i. were determined using the plaque assay. **a**–**c**, Effect of ddhC on three different ZIKV isolates: MR766 (Uganda 1947) (**a**), PRVABC59 (Puerto Rico; 2015) (**b**) or R103451 (Honduras; 2016) (**c**). Analysis of ZIKV titres indicates that 1 mM ddhC inhibits all three ZIKV isolates compared to 0 mM ddhC. However, reduction in virus titre is more prominent at 24 h.p.i. and 48 h.p.i. compared to 72 h.p.i. when using an MOI of 1.0. The antiviral effect of ddhC is more prominent at an MOI of 0.1. Data are mean ± s.d. from three biologically independent samples, *P* values from a two-way ANOVA with Dunnett's post hoc analysis.

nature research

Corresponding author(s): Steven C. Almo, Tyler L. Grove

Reporting Summary

Nature Research wishes to improve the reproducibility of the work that we publish. This form provides structure for consistency and transparency in reporting. For further information on Nature Research policies, see Authors & Referees and the Editorial Policy Checklist.

Statistical parameters

When statistical analyses are reported, confirm that the following items are present in the relevant location (e.g. figure legend, table legend, main text, or Methods section).

n/a	Confirmed	
☐	☒	The exact sample size (*n*) for each experimental group/condition, given as a discrete number and unit of measurement
☐	☒	An indication of whether measurements were taken from distinct samples or whether the same sample was measured repeatedly
☐	☒	The statistical test(s) used AND whether they are one- or two-sided *Only common tests should be described solely by name; describe more complex techniques in the Methods section.*
☐	☒	A description of all covariates tested
☐	☒	A description of any assumptions or corrections, such as tests of normality and adjustment for multiple comparisons
☐	☒	A full description of the statistics including central tendency (e.g. means) or other basic estimates (e.g. regression coefficient) AND variation (e.g. standard deviation) or associated estimates of uncertainty (e.g. confidence intervals)
☐	☒	For null hypothesis testing, the test statistic (e.g. *F*, *t*, *r*) with confidence intervals, effect sizes, degrees of freedom and *P* value noted *Give P values as exact values whenever suitable.*
☒	☐	For Bayesian analysis, information on the choice of priors and Markov chain Monte Carlo settings
☒	☐	For hierarchical and complex designs, identification of the appropriate level for tests and full reporting of outcomes
☒	☐	Estimates of effect sizes (e.g. Cohen's *d*, Pearson's *r*), indicating how they were calculated
☐	☒	Clearly defined error bars *State explicitly what error bars represent (e.g. SD, SE, CI)*

Our web collection on statistics for biologists may be useful.

Software and code

Policy information about availability of computer code

Data collection	Data generated using a 6410 or 6490 Agilent QQQ Mass Spec was analyzed and quantified using Agilent's Mass Hunter software package (ver. B0.4). The statistical analysis was performed using the analysis package in the GraphPad software Prism7 (ver. 7.0a). Gels were visualized by using a GE Healthcare Life Sciences PhosphorImager and quantified by using the ImageQuant TL software (ver. 7.0).
Data analysis	Data generated using a 6410 or 6490 Agilent QQQ Mass Spec was analyzed and quantified using Agilent's Mass Hunter software package (ver. B0.4). The statistical analysis was performed using the analysis package in the GraphPad software Prism7 (ver. 7.0a). Gels were visualized by using a GE Healthcare Life Sciences PhosphorImager and quantified by using the ImageQuant TL software (ver. 7.0).

For manuscripts utilizing custom algorithms or software that are central to the research but not yet described in published literature, software must be made available to editors/reviewers upon request. We strongly encourage code deposition in a community repository (e.g. GitHub). See the Nature Research guidelines for submitting code & software for further information.

Data

Policy information about availability of data

All manuscripts must include a data availability statement. This statement should provide the following information, where applicable:

- Accession codes, unique identifiers, or web links for publicly available datasets
- A list of figures that have associated raw data
- A description of any restrictions on data availability

Data available from the authors on request.

Field-specific reporting

Please select the best fit for your research. If you are not sure, read the appropriate sections before making your selection.

☒ Life sciences ☐ Behavioural & social sciences ☐ Ecological, evolutionary & environmental sciences

For a reference copy of the document with all sections, see nature.com/authors/policies/ReportingSummary-flat.pdf

Life sciences study design

All studies must disclose on these points even when the disclosure is negative.

Sample size	We chose n = 3 replicates because it allows for statistically relevant errors of the mean to be calculated
Data exclusions	No data was excluded
Replication	All attempts at replication succeeded
Randomization	Randomization is not relevant to enzyme kinetic assays. Transfections and viral infections of cells examine the response of entire populations and are not amenable to randomization.
Blinding	These studies did not involve human or animal participants and were not blinded.

Reporting for specific materials, systems and methods

Materials & experimental systems

n/a	Involved in the study
☒	☐ Unique biological materials
☒	☐ Antibodies
☒	☐ Eukaryotic cell lines
☒	☐ Palaeontology
☒	☐ Animals and other organisms
☒	☐ Human research participants

Methods

n/a	Involved in the study
☒	☐ ChIP-seq
☒	☐ Flow cytometry
☒	☐ MRI-based neuroimaging